STATISTICAL HADRONIZATION: SUCCESSES AND SOME OPEN ISSUES

Anton Andronic [a], Peter Braun-Munzinger [b,c,d]
Krzysztof Redlich [e], Johanna Stachel [c,d]

[a] Institut für Kernphysik, Universität Münster, 48149 Münster, Germany
[b] Research Division and EMMI, GSI Helmholtzzentrum für Schwerionenforschung
64291 Darmstadt, Germany
[c] Physikalisches Institut, Universität Heidelberg, 69120 Heidelberg, Germany
[d] Institute of Particle Physics and
Key Laboratory of Quark and Lepton Physics (MOE)
Central China Normal University, Wuhan 430079, China
[e] University of Wrocław, Institute of Theoretical Physics, 50-204 Wrocław, Poland

*Received 1 April 2026, accepted 9 April 2026,
published online 28 May 2026*

Hadron production in relativistic nuclear collisions is well described in the framework of the statistical hadronization model, over a broad range of collision energies. We outline this for hadrons composed of light (u, d, s) and heavy (charm and beauty) quarks, discuss recent findings relevant for understanding the phase structure of QCD, and formulate some open issues.

DOI:10.5506/APhysPolB.57.6-A5

1. Introduction

If one compresses or heats strongly interacting matter to higher densities and/or high temperatures, one expects [1–4] that quarks are no longer confined but can move over distances significantly larger than the size of a nucleon. Under very similar conditions, also a fundamental symmetry of QCD, the chiral symmetry that is spontaneously broken in hadronic and nuclear matter, is restored. Such a deconfined, chirally symmetric state of matter, the Quark–Gluon Plasma (QGP) [5], is likely to have existed in the Early Universe between the electroweak phase transition at picoseconds after the Big Bang and for up to 10 microseconds [6]. It can be studied experimentally and theoretically via collisions of nuclei at high energies [7, 8]. One stage in the complex dynamics of the system produced in heavy-ion collisions is that of the chemical freeze-out, at which the abundances of hadron species are fixed. Chemical freeze-out is addressed phenomenologically within the statistical hadronization model (SHM) [9–11]. The value of the pseudo-critical temperate T_c for the chiral crossover transition at vanishing μ_B is currently calculated in Lattice QCD (LQCD) to be 156.5 ± 1.5 MeV [12] and 158.0 ± 0.6 MeV [13]. The LQCD results also quantify a small decrease of T_c with increasing μ_B as long as $\mu_B \lesssim 400$ MeV [12–14]. Within this parameter range, the chiral transition is still of a crossover type [15]. The temperature for the deconfinement transition is more difficult to evaluate in LQCD due to the lack of an order parameter at finite quark masses. A recent extrapolation of the static quark entropy [16] puts the deconfinement transition line very close to the one for the chiral transition. The presence of new phases and possibly of a critical end point at values of μ_B around 600 MeV is currently theoretically discussed intensely and addressed experimentally, see very recent reviews [17, 18].

One of the consequences of confinement in QCD is that physical observables require a representation in terms of hadronic states. Indeed, as has been noted in the context of QCD thermodynamics (see, *e.g.*, [19] and references therein), the corresponding partition function Z can be very well approximated within the framework of the hadron resonance gas, as long as the temperature stays below T_c.

In a volume V, the grand canonical partition function for hadron species i is

$$\ln Z_i = \frac{V g_i}{2\pi^2} \int\limits_0^\infty \pm p^2 \mathrm{d}p \ln[1 \pm \exp(-(E_i - \mu_i)/T)] \tag{1}$$

with + for fermions and − for bosons, where $g_i = (2J_i + 1)$ is the spin degeneracy factor, T is the temperature, $E_i = \sqrt{p^2 + m_i^2}$ the total energy; $\mu_i = \mu_B B_i + \mu_{I_3} I_{3i} + \mu_S S_i + \mu_C C_i$ are the chemical potentials that ensure conservation (on average) of baryon, isospin, strangeness, and charm quantum numbers. Three initial conditions help fixing (I_{3i}, μ_S, μ_C)

(i) isospin stopping identical to baryon stopping: $I_3^{\mathrm{tot}} / \sum_i n_i I_{3i} = N_B^{\mathrm{tot}} / \sum_i n_i B_i$, with I_3^{tot} and N_B^{tot} as the isospin and baryon numbers of the system;

(ii) vanishing net initial strangeness: $\sum_i n_i S_i = 0$;

(iii) vanishing net initial charm content: $\sum_i n_i C_i = 0$.

One needs as input for the calculations knowledge of the complete hadron spectrum and the default constitutes what is listed by the PDG [20].

A consistent approach to interactions among hadrons is an implementation employing the S-matrix formulation of statistical mechanics with measured pion–nucleon phase shifts including, importantly, also repulsive and non-resonant components [21]. This accounts for the strongest contribution, the pion–nucleon interaction. Implementation of interactions in the strangeness sector is realized in [22]. For an interesting new contribution, see [23].

2. Statistical hadronization of light quarks

In practice, $T_{\rm CF}$, μ_B, and V, the parameters at chemical freeze-out are determined from a fit to the experimental data. For the most-central (0–10%) Pb–Pb collisions at the LHC, the best description of the ALICE data (see [24] and references therein) on yields of particles in one unit of rapidity at midrapidity, is obtained with $T_{\rm CF} = 156.6 \pm 1.7$ MeV, $\mu_B = 0.7 \pm 3.8$ MeV, and $V = 4175 \pm 380$ fm^3 (corresponding to a slice of one unit of rapidity, centered at midrapidity) [11, 21], shown in Fig. 1. The standard deviations quoted here are exclusively due to experimental uncertainties and do not reflect the systematic uncertainties connected with the model implementation. Further investigations have led to an order of magnitude improvement in the precision of $\mu_B = 0.7 \pm 0.45$ MeV [25], demonstrating that the central region at LHC energies is essentially baryon-free.

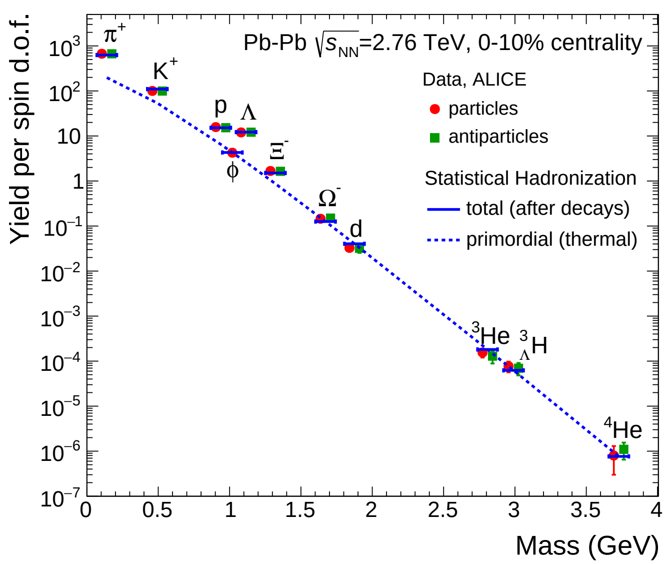

Fig. 1. Mass dependence of hadron yields divided by the spin degeneracy factor $(2J + 1)$, SHM best fit in comparison to the ALICE data. For the SHM, both the "total" yields, including strong and electromagnetic decays, and the "primordial" thermal yields are plotted. Figure taken from [26].

Very good agreement is obtained between the measured particle yields and SHM over nine orders of magnitude in abundance values, encompassing strange and non-strange mesons, baryons, including strange and multiply-strange hyperons, as well as light nuclei and hypernuclei, and their anti-particles. The initially observed overprediction of about 20% of the data by the model for proton and anti-proton yields (a deviation of 2.7σ) is entirely accounted for via the S-matrix treatment of the interactions [21] leading to an excellent fit with a $\chi^2_{\rm red} = 16.9/19$ (for consistency, with the S-matrix treatment, the excluded-volume correction is not applied anymore). It was recently shown that the addition (compared to what is listed by PDG [20]) of about 500 new states predicted by LQCD and the quark model does lead to a strong deterioration of the fit, while a restoration of the good fit quality at no change of the thermal parameters is observed when the S-matrix treatment is employed as well for this expanded hadron spectrum [27].

The thermal origin of all particles including light nuclei and anti-nuclei is particularly transparent when inspecting the dependence of their yields with particle mass, shown in Fig. 1. We note that the yields of the measured lightest mesons and baryons, (π, K, p, Λ) are substantially increased relative to their primordial thermal production by the resonance decay contributions (for pions, *e.g.*, the decay contribution amounts to 70% of the total yield). For the subset of light nuclei, the SHM predictions are, however, not affected by resonance decays. For these nuclei, due to their large masses, a small variation in temperature leads to a large variation in the yield, resulting in a relatively precise determination of the freeze-out temperature $T_{\rm nuclei} = 159 \pm 5$ MeV, well consistent with the value of $T_{\rm CF}$ extracted above.

The rapidity densities of light (anti-)nuclei and hypernuclei were actually predicted [28], based on the systematics of hadron production at lower energies. It is nevertheless remarkable that such loosely bound objects (the deuteron binding energy is 2.2 MeV, much less than $T_{\rm CF} \approx T_{\rm c} \approx 157$ MeV) are produced at temperatures very close to that of the phase boundary at LHC energy, implying that any further evolution of the fireball has to be close to isentropic. The detailed production mechanism for loosely bound states remains an open question (see recent review [29]). One possibility is that such objects, at QGP hadronization, are produced as compact, colorless droplets of quark matter with quantum numbers of the final-state hadrons [11] (see discussion below).

The thermal nature of particle production in ultra-relativistic nuclear collisions has been experimentally verified not only at LHC energy, but also at the lower energies of the RHIC, SPS, and AGS accelerators. The essential difference is that, at these lower energies, the matter–anti-matter symmetry observed at the LHC is lifted, implying non-vanishing values of the chemical potentials. Furthermore, in central collisions at energies below $\sqrt{s_{NN}} \approx 6$ GeV, the cross section for the production of strange-hadrons decreases

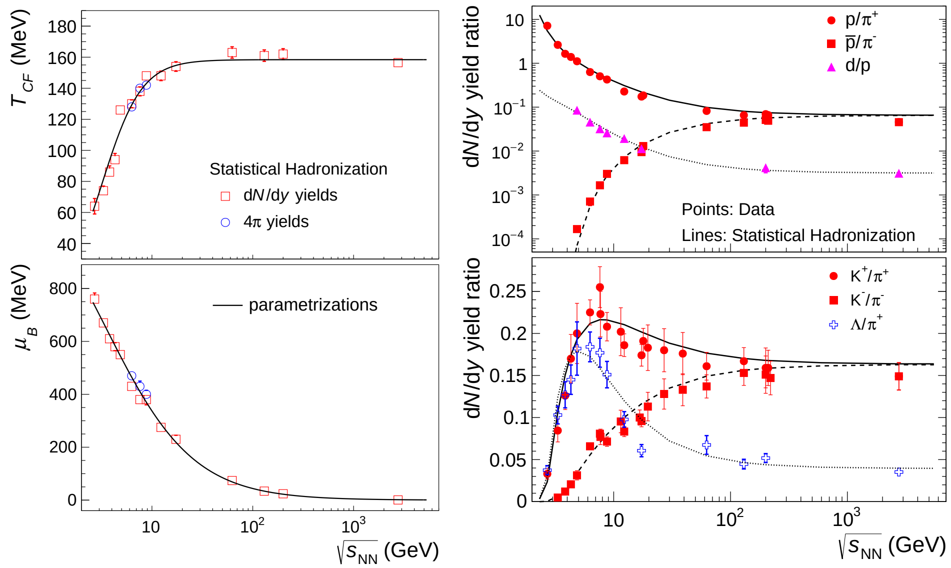

Fig. 2. Left: Energy dependence of the chemical freeze-out parameters $T_{\rm CF}$ and μ_B. The results are obtained from the SHM analysis of hadron yields (at midrapidity, dN/dy, and in full phase space, 4π) for central collisions at different energies. Right: Collision energy dependence of the relative abundance of several hadron species (the data are compiled in [30, 31]). Figures taken from [11].

rapidly, with the result that the average strange hadron yields per collision can be significantly below unity. In this situation, one needs to implement exact strangeness conservation, applying canonical thermodynamics [9, 32, 33]. Similar considerations apply to the description of particle yields in peripheral nuclear and elementary collisions.

While μ_B decreases smoothly with increasing energy, the dependence of $T_{\rm CF}$ on energy exhibits a striking feature which is illustrated in Fig. 2 (left): $T_{\rm CF}$ increases with increasing energy from about 60 MeV to a saturation for $\sqrt{s_{NN}} > 20$ GeV, of about 158 MeV, when averaging over all experiments. The saturation of $T_{\rm CF}$ observed in Fig. 2 lends support to the earlier proposal [34–36] that, at least at high energies, the chemical freeze-out temperature is very close to the QCD hadronization temperature [37], implying a direct connection between data from relativistic nuclear collisions and the QCD phase boundary. Hagedorn noted long ago [38] that hadronic matter cannot be heated beyond a certain limit, but the saturation observed here indicates a different boundary. The parametrizations shown in Fig. 2 are: $T_{\rm CF} = T_{\rm CF}^{\rm lim}/(1+\exp(2.60-\ln(\sqrt{s_{NN}})/0.45))$ and $\mu_B = a/(1+0.288\sqrt{s_{NN}})$, with $\sqrt{s_{NN}}$ in GeV, the 'limiting temperature' $T_{\rm CF}^{\rm lim} = 158.4 \pm 1.4$ MeV, and $a = 1307.5$ MeV.

To illustrate how well the thermal description of particle production in central nuclear collisions works, we show also in Fig. 2 (right), the energy dependence of the relative abundance of several hadron species along with the prediction using the SHM and the parametrized evolution of the parameters. In particular, the maxima (occurring at slightly different c.m. energies) in the K^+/π^+ and Λ/π^+ ratios are naturally explained [37] as the interplay between the energy dependence of $T_{\rm CF}$ and μ_B and the consequence of strangeness conservation. Deuterons are also well reproduced (see discussion below).

Since the statistical hadronization analysis at each collision energy yields a pair of ($T_{\rm CF}$, μ_B) values, these points can be entered into the phase diagram of QCD shown in Fig. 3. Note that the points at low temperature and high μ_B seem to converge towards the value for the ground-state nuclear matter ($\mu_B \simeq 930$ MeV). At high collision energies, the points are very close to the pseudo-critical line for the chiral phase transition (and deconfinement) [12, 13, 16].

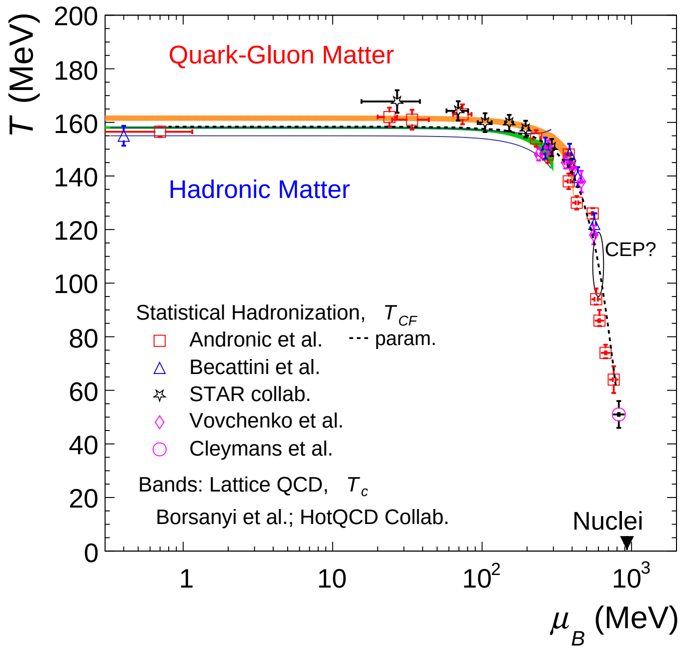

Fig. 3. Phase diagram of strongly interacting matter constructed from chemical freeze-out points for central collisions at different energies, extracted from experimental data sets in our own (squares) and other similar analyses [31, 39–41] is compared to predictions from LQCD [12, 13, 16] shown as bands. For the location of a possible critical endpoint (CEP), see [17].

3. Extension to hadrons with heavy quarks

There is now significant experimental information, from relativistic nuclear collisions, not only on the production of hadrons composed of light (u, d, s) valence quarks, but also of open and hidden charm and beauty hadrons. In particular, there is good evidence, mainly from results obtained at the CERN Large Hadron Collider (LHC) [42–44], that charm quarks reach a large degree of thermal equilibrium, although charm quarks in the system are initially chemically far out of equilibrium. This is supported by heavy-quark diffusion coefficients from LQCD [45, 46]. A strong indication for equilibration is the fact that J/ψ mesons participate in the collective, anisotropic hydrodynamic expansion [47, 48].

To microscopically understand the production mechanism of charmed hadrons for systems ranging from *pp* to Pb–Pb, various forms of quark coalescence models have been developed [49–52]. This provides a natural way to study the dependence of production yields on hadron size and, hence, may help to settle the still open question of whether the many exotic hadrons that have been observed recently are compact multi-quark states or hadronic molecules (see [53, 54] and references therein). Conceptual difficulties with this approach are that energy is not conserved in the coalescence process and that color neutralization at hadronization requires additional assumptions about quark correlations in the QGP [55].

Another approach, named SHMc, has been formulated by the extension of the SHM to also incorporate charm quarks. This was first proposed in [56] and developed further in [11, 43, 57, 58] to include all hadrons with hidden and open charm. The key idea is based on the recognition that, contrary to what happens in the (u, d, s) sector, the heavy (mass ~ 1.2 GeV) charm quarks are not thermally produced even at LHC energy. Rather, production takes place in initial hard collisions. The produced charm quarks then thermalize in the hot fireball, but the total number of charm quarks is conserved during the evolution of the fireball [58] since charm quark annihilation is very small. In essence, this implies that charm quarks can be treated like impurities. Their thermal description then requires the introduction of a charm fugacity g_c [43, 56]. The value of g_c is not a free parameter but experimentally determined by measurement of the total charm cross section. For central Pb–Pb collisions at LHC energy, $g_c \approx 30$ [43]. The charmed hadrons are, in the SHMc, all formed at the phase boundary, *i.e.* at hadronization, in the same way as all (u, d, s) hadrons, only with the boundary condition that all charm quarks present in the QGP materialize in hadrons (as warranted by g_c).

In [44], it is demonstrated that, with that choice, the measured yield for J/ψ mesons is very well reproduced along with the yield of all light-flavor hadrons. The uncertainty in the prediction is mainly caused by the uncertainty in the total charm cross section in Pb–Pb collisions. We note here that the excellent agreement of charmed-hadron yields with those computed with the SHMc implies that charm quarks, and consequently charmonia, are unbound inside the QGP; in fact, their final yields at full LHC energy exhibit enhancement compared to expectations using collision scaling from pp collisions, contrary to the original predictions based on [59]. For a detailed discussion, see [11].

For the description of yields of charmonia, feeding from excited charmonia is very small due to their strong Boltzmann suppression. For open charm mesons and baryons, this is not the case, and feeding from excited D^*, Λ_c^*, and Σ_c^* is an essential ingredient for the description of open charm hadrons [43]. Even though the experimental mass spectrum of excited open charm hadrons is not complete, in particular in the baryon sector, the prediction of yields for D mesons and Λ_c baryons compares very well with the measurements[1], both concerning transverse momentum and centrality dependence.

A particularly transparent way to look at the data for Pb–Pb collisions is obtained by analyzing the centrality dependence of the yield ratio $(J/\psi)/D^0$ and comparing the results to the predictions of the SHMc. Recently, both the D^0 and J/ψ production cross sections have been well measured down to $p_{\mathrm{t}} = 0$. The yield ratio $(J/\psi)/D_0$ is reproduced with very good precision for both measured centralities, as demonstrated in Fig. 4. This result lends strong support to the assumption that open and hidden charm states are both produced by statistical hadronization at the phase boundary. A more extensive comparison between SHMc and data for open charm hadrons is shown in [43, 62].

From the successful comparison of measured yields for the production of (u, d, s) as well as open and hidden charm hadrons obtained from the SHM or SHMc with essentially only the temperature as a free parameter at LHC energies, one may draw a number of important conclusions.

— First, we note that hadron production in relativistic nuclear collisions is described quantitatively by the chemical freeze-out parameters (T_{CF}, μ_B). Note that the fireball volume appearing in the partition function is determined by normalization to the measured number of primary charged particles. At least for energies $\sqrt{s_{NN}} \geq 10$ GeV, these

[1] For Λ_c baryons, one has to augment the currently measured charm-baryon spectrum to account for the large number of additional states predicted by LQCD to achieve agreement with experimental data [61].

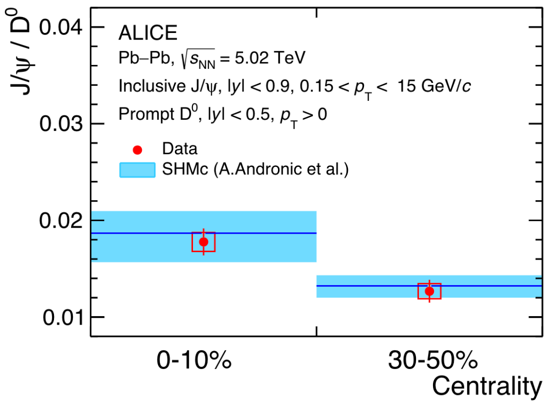

Fig. 4. J/ψ to D^0 ratio measured in Pb–Pb collisions at the LHC and predicted by the Statistical Hadronization Model with charm SHMc. Figure from [60].

freeze-out parameters agree with good precision with the results from LQCD for the location of the chiral crossover transition. Under these conditions, hadronization is independent of particle species and only dependent on the values of T and μ_B at the phase boundary. At LHC energy, the chemical potentials vanish, and only $T = T_c$ is needed to describe hadronization.

— The mechanism implemented in the SHMc for the production of charmed hadrons implies that these particles are produced from uncorrelated, thermalized charm quarks as is expected for a strongly coupled, deconfined QGP (see also the discussion in [43]). At LHC energy, where chemical freeze-out takes place for central Pb–Pb collisions in a volume per unit rapidity of $V \approx 5000$ fm^3, this implies that charm quarks can travel over linear distances of order 10 fm (see [11, 43] for more detail). This result provides strong evidence for deconfinement in the charm sector. Recent theoretical studies provide some arguments for the presence of a confined phase at temperatures above the hadron-resonance-gas phase but below the QGP phase [63, 64]. The observation of deconfined charm quarks above T_c does not lend support for the existence of such a phase, since colorless charmonium cannot be formed from colored charm and anti-charm quarks in absence of gluons.

Future measurement campaigns at the LHC will yield detailed information on the production cross sections of hadrons with multiple charm quarks as well as excited charmonia. The predictions from the SHMc for the relevant cross sections exhibit a rather dramatic hierarchy of enhancements [43] for such processes. Experimental tests of these predictions would lead to a fundamental understanding of confinement/deconfinement and hadronization. The vision is to obtain, from the measured charmonium spectrum compared to SHMc, a deconfinement temperature similar in spirit to the above cited freeze-out temperature for nuclei.

4. Some open issues

We have demonstrated that the SHM and SHMc approaches provide an excellent description of hadron production in relativistic nuclear collisions from $\sqrt{s_{NN}} = 3$ GeV into the multi-TeV range. Recently, there has been increased interest in searching for quark–gluon plasma signatures also in light systems such as pA and pp collisions [65]. This has led to investigations of SHMc predictions also for these systems [66] and established new systematics which is rather well visible in the available data, with the exception of the D_s^0 meson, whose yield is unexpectedly suppressed by about a factor of 2 compared to SHMc predictions. Furthermore, the degree of equilibration reached in the light systems has not yet been well determined.

The detailed production mechanism for composite objects such as light nuclei and hyper-nuclei has not yet been fully established, despite significant experimental efforts. As cases in point, we note that the system size dependence of the loosely bound hyper-triton which for pp collisions is better understood in a coalescence framework, while ^{4}He and mass-4 hypernucleus production in heavy systems is well described in the SHM approach. We note in this context that a possible connection between coalescence models and SHM was already recognized more than 30 years ago [67, 68], see also a recent study in [69]. Clearly, very loosely bound objects such as hyper-triton with a radius of order of 10 fm cannot survive even the dilute hadronic phase after chemical freeze-out. In [11], it was then speculated that such objects are first produced as compact (multi-quark) clusters with mass and quantum number of the final state such as hyper-triton and only significantly later evolve into the full nuclear wave function. How this evolution takes place is, however, not understood. On the other hand, hyper-triton cannot directly coalesce into the fully formed large object as the coalescence process has to take place via the strong interaction which is very short range (1–2 fm). So in both models, the initial configuration has to be compact. The importance of this aspect is not currently taken into account in the coalescence approach.

A possible way of how to deal in the SHM with the production of objects whose size is comparable to or even much larger than the size of the fireball formed in the collision was recently proposed in a schematic way in [70]. This mechanism was very recently implemented into our version of the SHM but indeed does not lead to agreement with the measured system-size dependence of the production yields of light nuclei [71], where the canonical suppression is sufficient to describe the experimental data.

Finally, we recognize the efforts by Cohen and collaborators [72, 73] to shed light on the 'light nucleus puzzle' but do not share their understanding of the non-equilibrium dilute hadronic phase after chemical freeze-out in SHM.

K.R. acknowledges support from the National Science Centre (NCN), Poland, under OPUS grant No. 2022/45/B/ST2/01527, and of the Polish Ministry of Science and Higher Education. This work is part of and supported by the DFG Collaborative Research Centre, SFB1225/ ISOQUANT.

REFERENCES

[1] N. Itoh, «Hydrostatic Equilibrium of Hypothetical Quark Stars», *Prog. Theor. Phys.* **44**, 291 (1970).

[2] J.C. Collins, M. Perry, «Superdense Matter: Neutrons or Asymptotically Free Quarks?», *Phys. Rev. Lett.* **34**, 1353 (1975).

[3] N. Cabibbo, G. Parisi, «Exponential hadronic spectrum and quark liberation», *Phys. Lett. B* **59**, 67 (1975).

[4] G. Chapline, M. Nauenberg, «Asymptotic freedom and the baryon–quark phase transition», *Phys. Rev. D* **16**, 450 (1977).

[5] E.V. Shuryak, «Quark–gluon plasma and hadronic production of leptons, photons and psions», *Phys. Lett. B* **78**, 150 (1978).

[6] D. Boyanovsky, H. de Vega, D. Schwarz, «Phase Transitions in the Early and the Present Universe», *Annu. Rev. Nucl. Part. Sci.* **56**, 441 (2006), `arXiv:hep-ph/0602002`.

[7] W. Busza, K. Rajagopal, W. van der Schee, «Heavy Ion Collisions: The Big Picture, and the Big Questions», *Annu. Rev. Nucl. Part. Sci.* **68**, 339 (2018), `arXiv:1802.04801 [hep-ph]`.

[8] P. Braun-Munzinger, V. Koch, T. Schäfer, J. Stachel, «Properties of hot and dense matter from relativistic heavy ion collisions», *Phys. Rep.* **621**, 76 (2016), `arXiv:1510.00442 [nucl-th]`.

[9] P. Braun-Munzinger, K. Redlich, J. Stachel, «Particle Production in Heavy Ion Collisions», in: R.C. Hwa, X.N. Wang (Eds.) «Quark–Gluon Plasma 3», *World Scientific Publishing*, 2003, pp. 491–599, `arXiv:nucl-th/0304013`.

[10] A. Andronic, P. Braun-Munzinger, J. Stachel, «Hadron production in central nucleus–nucleus collisions at chemical freeze-out», *Nucl. Phys. A* **772**, 167 (2006), `arXiv:nucl-th/0511071`.

[11] A. Andronic, P. Braun-Munzinger, K. Redlich, J. Stachel, «Decoding the phase structure of QCD via particle production at high energy», *Nature* **561**, 321 (2018), arXiv:1710.09425 [nucl-th].

[12] HotQCD Collaboration (A. Bazavov *et al.*), «Chiral crossover in QCD at zero and non-zero chemical potentials», *Phys. Lett. B* **795**, 15 (2019), arXiv:1812.08235 [hep-lat].

[13] S. Borsanyi *et al.*, «QCD Crossover at Finite Chemical Potential from Lattice Simulations», *Phys. Rev. Lett.* **125**, 052001 (2020), arXiv:2002.02821 [hep-lat].

[14] C. Bonati *et al.*, «Curvature of the pseudocritical line in QCD: Taylor expansion matches analytic continuation», *Phys. Rev. D* **98**, 054510 (2018), arXiv:1805.02960 [hep-lat].

[15] Y. Aoki *et al.*, «The order of the quantum chromodynamics transition predicted by the standard model of particle physics», *Nature* **443**, 675 (2006), arXiv:hep-lat/0611014.

[16] S. Borsanyi *et al.*, «QCD deconfinement transition line up to $\mu_B = 400$ MeV from finite volume lattice simulations», *Phys. Rev. D* **110**, 114507 (2024), arXiv:2410.06216 [hep-lat].

[17] C.S. Fischer, J.M. Pawlowski, «Phase structure and observables at high densities from first principles QCD», arXiv:2603.11135 [hep-ph].

[18] P. Braun-Munzinger, A. Rustamov, N. Xu, «The phase structure of QCD: Fluctuations and Correlations», arXiv:2601.18666 [nucl-ex].

[19] A. Bazavov *et al.*, «QCD equation of state to $\mathcal{O}(\mu_B^6)$ from lattice QCD», *Phys. Rev. D* **95**, 054504 (2017), arXiv:1701.04325 [hep-lat].

[20] Particle Data Group (P. Zyla *et al.*), «Review of Particle Physics», *Prog. Theor. Exp. Phys.* **2020**, 083C01 (2020).

[21] A. Andronic *et al.*, «The thermal proton yield anomaly in Pb–Pb collisions at the LHC and its resolution», *Phys. Lett. B* **792**, 304 (2019), arXiv:1808.03102 [hep-ph].

[22] J. Cleymans, P.M. Lo, K. Redlich, N. Sharma, «Multiplicity dependence of (multi)strange baryons in the canonical ensemble with phase shift corrections», *Phys. Rev. C* **103**, 014904 (2021), arXiv:2009.04844 [hep-ph].

[23] S. Yasui, S.H. Lee, P.M. Lo, C. Sasaki, «New nonet scalar mesons and glueballs: the mass spectra and the production yields in relativistic heavy ion collisions», arXiv:2603.13764 [hep-ph].

[24] ALICE Collaboration (S. Acharya *et al.*), «Production of ^{4}He and $^4\overline{\text{He}}$ in Pb–Pb collisions at $\sqrt{s_{NN}} = 2.76$ TeV at the LHC», *Nucl. Phys. A* **971**, 1 (2018), arXiv:1710.07531 [nucl-ex].

[25] ALICE Collaboration (S. Acharya *et al.*), «Measurements of Chemical Potentials in Pb–Pb Collisions at $\sqrt{s_{NN}} = 5.02$ TeV», *Phys. Rev. Lett.* **133**, 092301 (2024), arXiv:2311.13332 [nucl-ex].

[26] A. Andronic, P. Braun-Munzinger, K. Redlich, J. Stachel, «Hadron yields in central nucleus–nucleus collisions, the statistical hadronization model and the QCD phase diagram», in: «Proceedings of the workshop "Criticality in QCD and the Hadron Resonance Gas"», Wroclaw (online), Poland, 29–31 July, 2020, arXiv:2101.05747 [nucl-th].

[27] A. Andronic *et al.*, «Influence of modified light-flavor hadron spectra on particle yields in the statistical hadronization model», *Nucl. Phys. A* **1010**, 122176 (2021), arXiv:2011.03826 [nucl-th].

[28] A. Andronic, P. Braun-Munzinger, J. Stachel, H. Stöcker, «Production of light nuclei, hypernuclei and their antiparticles in relativistic nuclear collisions», *Phys. Lett. B* **697**, 203 (2011), arXiv:1010.2995 [nucl-th].

[29] P. Braun-Munzinger, B. Dönigus, «Loosely-bound objects produced in nuclear collisions at the LHC», *Nucl. Phys. A* **987**, 144 (2019), arXiv:1809.04681 [nucl-ex].

[30] A. Andronic, «An overview of the experimental study of quark–gluon matter in high-energy nucleus–nucleus collisions», *Int. J. Mod. Phys. A* **29**, 1430047 (2014), arXiv:1407.5003 [nucl-ex].

[31] STAR Collaboration (L. Adamczyk *et al.*), «Bulk properties of the medium produced in relativistic heavy-ion collisions from the beam energy scan program», *Phys. Rev. C* **96**, 044904 (2017), arXiv:1701.07065 [nucl-ex].

[32] R. Hagedorn, K. Redlich, «Statistical Thermodynamics in Relativistic Particle and Ion Physics: Canonical or Grand Canonical?», *Z. Phys. C* **27**, 541 (1985).

[33] S. Hamieh, K. Redlich, A. Tounsi, «Canonical description of strangeness enhancement from p–A to Pb–Pb collisions», *Phys. Lett. B* **486**, 61 (2000), arXiv:hep-ph/0006024.

[34] P. Braun-Munzinger, J. Stachel, «Dynamics of ultrarelativistic nuclear collisions with heavy beams: An experimental overview», *Nucl. Phys. A* **638**, 3 (1998), arXiv:nucl-ex/9803015.

[35] R. Stock, «The parton to hadron phase transition observed in Pb+Pb collisions at 158 GeV per nucleon», *Phys. Lett. B* **456**, 277 (1999), arXiv:hep-ph/9905247.

[36] P. Braun-Munzinger, J. Stachel, C. Wetterich, «Chemical freezeout and the QCD phase transition temperature», *Phys. Lett. B* **596**, 61 (2004), arXiv:nucl-th/0311005.

[37] A. Andronic, P. Braun-Munzinger, J. Stachel, «Thermal hadron production in relativistic nuclear collisions: The hadron mass spectrum, the horn, and the QCD phase transition», *Phys. Lett. B* **673**, 142 (2009); *Erratum: ibid.* **678**, 516 (2009), arXiv:0812.1186 [nucl-th].

[38] R. Hagedorn, «Statistical thermodynamics of strong interactions at high-energies», *Nuovo Cim. Suppl.* **3**, 147 (1965).

[39] J. Cleymans, H. Oeschler, K. Redlich, «Influence of impact parameter on thermal description of relativistic heavy ion collisions at (1–2)A GeV», *Phys. Rev. C* **59**, 1663 (1999), arXiv:nucl-th/9809027.

[40] V. Vovchenko, V.V. Begun, M.I. Gorenstein, «Hadron multiplicities and chemical freeze-out conditions in proton–proton and nucleus–nucleus collisions», *Phys. Rev. C* **93**, 064906 (2016), arXiv:1512.08025 [nucl-th].

[41] F. Becattini, J. Steinheimer, R. Stock, M. Bleicher, «Hadronization conditions in relativistic nuclear collisions and the QCD pseudo-critical line», *Phys. Lett. B* **764**, 241 (2017), arXiv:1605.09694 [nucl-th].

[42] ALICE Collaboration, (S. Acharya *et al.*), «Prompt D^0, D^+, and D^{*+} production in Pb–Pb collisions at $\sqrt{s_{NN}} = 5.02$ TeV», *J. High Energy Phys.* **2022**, 174 (2022), arXiv:2110.09420 [nucl-ex].

[43] A. Andronic *et al.*, «The multiple-charm hierarchy in the statistical hadronization model», *J. High Energy Phys.* **2021**, 035 (2021), arXiv:2104.12754 [hep-ph].

[44] A. Andronic *et al.*, «Transverse momentum distributions of charmonium states with the statistical hadronization model», *Phys. Lett. B* **797**, 134836 (2019), arXiv:1901.09200 [nucl-th].

[45] L. Altenkort *et al.*, «Heavy quark momentum diffusion from the lattice using gradient flow», *Phys. Rev. D* **103**, 014511 (2021), arXiv:2009.13553 [hep-lat].

[46] HotQCD Collaboration (L. Altenkort *et al.*), «Heavy Quark Diffusion from 2+1 Flavor Lattice QCD with 320 MeV Pion Mass», *Phys. Rev. Lett.* **130**, 231902 (2023), arXiv:2302.08501 [hep-lat].

[47] ALICE Collaboration (E. Abbas *et al.*), «J/ψ elliptic flow in Pb–Pb Collisions at $\sqrt{s_{NN}} = 2.76$ TeV», *Phys. Rev. Lett.* **111**, 162301 (2013), arXiv:1303.5880 [nucl-ex].

[48] M. He, B. Wu, R. Rapp, «Collectivity of J/ψ Mesons in Heavy-Ion Collisions», *Phys. Rev. Lett.* **128**, 162301 (2022), arXiv:2111.13528 [nucl-th].

[49] S. Cho *et al.*, «Charmed hadron production in an improved quark coalescence model», *Phys. Rev. C* **101**, 024909 (2020), arXiv:1905.09774 [nucl-th].

[50] ExHIC Collaboration (S. Cho *et al.*), «Exotic hadrons from heavy ion collisions», *Prog. Part. Nucl. Phys.* **95**, 279 (2017), arXiv:1702.00486 [nucl-th].

[51] K. Zhou, N. Xu, Z. Xu, P. Zhuang, «Medium effects on charmonium production at ultrarelativistic energies available at the CERN Large Hadron Collider», *Phys. Rev. C* **89**, 054911 (2014), arXiv:1401.5845 [nucl-th].

[52] V. Greco, C. Ko, R. Rapp, «Quark coalescence for charmed mesons in ultrarelativistic heavy-ion collisions», *Phys. Lett. B* **595**, 202 (2004), arXiv:nucl-th/0312100.

[53] G. Aarts *et al.*, «Heavy-flavor production and medium properties in high-energy nuclear collisions — What next?», *Eur. Phys. J. A* **53**, 93 (2017), arXiv:1612.08032 [nucl-th].

[54] L. Maiani, A. Pilloni, «GGI Lectures on Exotic Hadrons», arXiv:2207.05141 [hep-ph].

[55] T. Song, G. Coci, «Prerequisites for heavy quark coalescence in heavy-ion collisions», *Nucl. Phys. A* **1028**, 122539 (2022), `arXiv:2104.10987 [nucl-th]`.

[56] P. Braun-Munzinger, J. Stachel, «(Non)thermal aspects of charmonium production and a new look at J/ψ suppression», *Phys. Lett. B* **490**, 196 (2000), `arXiv:nucl-th/0007059`.

[57] A. Andronic, P. Braun-Munzinger, K. Redlich, J. Stachel, «Statistical hadronization of charm in heavy-ion collisions at SPS, RHIC and LHC», *Phys. Lett. B* **571**, 36 (2003), `arXiv:nucl-th/0303036`.

[58] A. Andronic, P. Braun-Munzinger, K. Redlich, J. Stachel, «Statistical hadronization of heavy quarks in ultra-relativistic nucleus–nucleus collisions», *Nucl. Phys. A* **789**, 334 (2007), `arXiv:nucl-th/0611023`.

[59] T. Matsui, H. Satz, «J/ψ suppression by quark–gluon plasma formation», *Phys. Lett. B* **178**, 416 (1986).

[60] ALICE Collaboration (S. Acharya *et al.*), «Measurements of inclusive J/ψ production at midrapidity and forward rapidity in Pb–Pb collisions at $\sqrt{s_{NN}} = 5.02$ TeV», *Phys. Lett. B* **849**, 138451 (2024), `arXiv:2303.13361 [nucl-ex]`.

[61] A. Andronic *et al.*, «Transverse dynamics of charmed hadrons in ultra-relativistic nuclear collisions», *J. High Energy Phys.* **2024**, 229 (2024), `arXiv:2308.14821 [hep-ph]`.

[62] ALICE Collaboration (S. Acharya *et al.*), «The ALICE experiment: a journey through QCD», *Eur. Phys. J. C* **84**, 813 (2024), `arXiv:2211.04384 [nucl-ex]`.

[63] T.D. Cohen, L.Y. Glozman, «Large N_c QCD phase diagram at $\mu_B = 0$», *Eur. Phys. J. A* **60**, 171 (2024), `arXiv:2311.07333 [hep-ph]`.

[64] Y. Fujimoto, K. Fukushima, Y. Hidaka, L. McLerran, «New state of matter between the hadronic phase and the quark–gluon plasma?», *Phys. Rev. D* **112**, 074006 (2025), `arXiv:2506.00237 [hep-ph]`.

[65] J.F. Grosse-Oetringhaus, U.A. Wiedemann, «A Decade of Collectivity in Small Systems», `arXiv:2407.07484 [hep-ex]`.

[66] P. Braun-Munzinger, K. Redlich, N. Sharma, J. Stachel, «Emergence of new systematics for open charm production in high energy collisions», *J. High Energy Phys.* **2025**, 058 (2025), `arXiv:2408.07496 [hep-ph]`.

[67] A.J. Baltz *et al.*, «Strange cluster formation in relativistic heavy ion collisions», *Phys. Lett. B* **325**, 7 (1994).

[68] P. Braun-Munzinger, J. Stachel, «Production of strange clusters and strange matter in nucleus–nucleus collisions at the AGS», *J. Phys. G: Nucl. Part. Phys.* **21**, L17 (1995), `arXiv:nucl-th/9412035`.

[69] T. Reichert *et al.*, «Energy dependence of light hypernuclei production in heavy-ion collisions from a coalescence and statistical-thermal model perspective», *Phys. Rev. C* **107**, 014912 (2023), `arXiv:2210.11876 [nucl-th]`.

[70] B. Müller, «SQM2022: Theoretical Summary», *EPJ Web Conf.* **276**, 06017 (2023), arXiv:2209.00070 [hep-ph].

[71] A. Andronic, P. Braun-Munzinger, H. Brunßen, J. Stachel, «The Effect of Nuclear Size on the Production of Nuclei and Hypernuclei in the Statistical Hadronization Model», in preparation, 2026.

[72] Y. Cai, T.D. Cohen, B.A. Gelman, Y. Yamauchi, «Yields of weakly-bound light nuclei as a probe of the statistical hadronization model», *Phys. Rev. C* **100**, 024911 (2019), arXiv:1905.02753 [nucl-th].

[73] T. Cohen, M. Pradeep, «Hypertriton puzzle in relativistic heavy-ion collisions», *Phys. Rev. C* **111**, 054917 (2025), arXiv:2410.05569 [nucl-th].